

Title	Epitaxial growth and optical properties of semipolar (11 $\bar{2}$ ) GaN and InGaN/GaN quantum wells on GaN bulk substrates
Author(s)	Ueda, M; Kojima, K; Funato, M; Kawakami, Y; Narukawa, Y; Mukai, T
Citation	APPLIED PHYSICS LETTERS (2006), 89(21)
Issue Date	2006-11-20
URL	<a href="http://hdl.handle.net/2433/50131">http://hdl.handle.net/2433/50131</a>
Right	Copyright 2006 American Institute of Physics. This article may be downloaded for personal use only. Any other use requires prior permission of the author and the American Institute of Physics.
Type	Journal Article
Textversion	publisher; none

## Epitaxial growth and optical properties of semipolar (11 $\bar{2}$ 2) GaN and InGaN/GaN quantum wells on GaN bulk substrates

M. Ueda, K. Kojima, M. Funato,<sup>a)</sup> and Y. Kawakami

*Department of Electronic Science and Engineering, Kyoto University, Kyoto 615-8510, Japan*

Y. Narukawa and T. Mukai

*Nitride Semiconductor Research Laboratory, Nichia Corporation, Tokushima 774-8601, Japan*

(Received 30 August 2006; accepted 11 October 2006; published online 21 November 2006)

GaN and InGaN/GaN multiple quantum well (MQW) were grown on semipolar (11 $\bar{2}$ 2) GaN bulk substrates by metal organic vapor phase epitaxy. The GaN homoepitaxial layer has an atomically flat surface. Optical reflection measurements reveal polarization anisotropy for the *A*, *B*, and *C* excitons. Free *A* excitons dominate the photoluminescence (PL) spectrum at 10 K and are accompanied by a weaker, sharp doublet emission due to neutral donor-bound excitons. The InGaN/GaN MQW grown on a GaN homoepitaxial layer involves fast radiative recombination processes. The PL decay monitored at 428 nm can be fitted with a double exponential curve, which has lifetimes of 46 and 142 ps at 10 K. These values are two orders of magnitude shorter than those in conventional *c*-oriented QWs and are attributed to the weakened internal electric field. The emissions from GaN and MQW polarize along the [1 $\bar{1}$ 00] direction with polarization degrees of 0.46 and 0.69, respectively, due to the low crystal symmetry. © 2006 American Institute of Physics.

[DOI: 10.1063/1.2397029]

Light emitters based on nitride semiconductors typically consist of *c*-oriented quantum wells (QWs), where the quantum confinement Stark effect is caused by piezoelectric and spontaneous polarizations, which lower the optical transition probability.<sup>1</sup> To circumvent this issue, several groups have tried to fabricate InGaN/GaN and GaN/AlGaIn QWs on nonpolar planes such as {10 $\bar{1}$ 0} (*m* plane) (Ref. 2) and {11 $\bar{2}$ 0} (*a* plane).<sup>3</sup> However, the layers contain numerous nonradiative recombination centers because it is difficult to grow perfect high quality crystals in nonpolar directions.

Alternatively, there is an increasing interest in semipolar planes, which are tilted with respect to the *c* plane,<sup>4-9</sup> because a reduced or even negligible electric field is theoretically expected.<sup>10,11</sup> We have found that the {11 $\bar{2}$ 2} plane is promising for low internal electric fields when these planes naturally appear as microfacets through the regrowth process on *c*-oriented GaN templates.<sup>4</sup> (This structure is being developed as a multicolor emitter.<sup>5,6</sup>) However, planar, semipolar nitride layers and devices grown on foreign substrates suffer from a high density of threading dislocations and rough surfaces,<sup>7-9</sup> which has led us to believe that, if high quality GaN substrates were available, device performances would be drastically improved. In fact, we have recently fabricated high quality InGaN/GaN light emitting diodes on semipolar {11 $\bar{2}$ 2} GaN bulk substrates.<sup>12</sup> This study investigates the growth characteristics and fundamental optical properties of semipolar (11 $\bar{2}$ 2) GaN and InGaN/GaN QWs.

Figure 1 illustrates the crystal structure of GaN with a (11 $\bar{2}$ 2) surface. In terms of polarization anisotropy in the optical properties, the key in-plane directions are the [1 $\bar{1}$ 00] direction, which is perpendicular to the *c* axis, and [1 $\bar{1}$ 23],

which is parallel to the projection of the *c* axis on the (11 $\bar{2}$ 2) plane and perpendicular to [1 $\bar{1}$ 00]. Semipolar {11 $\bar{2}$ 2} GaN substrates used in this study were equivalent to those in the previous study.<sup>12</sup> In this study, all the structures were grown on the (11 $\bar{2}$ 2) plane by low-pressure (300 Torr) metal organic vapor phase epitaxy. The GaN layers were directly grown on the substrates at high temperatures, and InGaN/GaN multiple QWs (MQWs) followed.

Let us begin by discussing GaN homoepitaxy. Two GaN layers were grown at different temperatures of ~1050 and 975 °C. The optimal growth temperature for conventional *c*-oriented GaN on sapphire is 1050 °C, which creates GaN surfaces with step and terrace structures. The surface morphologies of these GaN layers as well as that of an as-received bulk GaN substrate were observed by atomic force microscopy (AFM) and are shown in Fig. 2. The surface of the GaN substrate is covered with numerous dotlike structures [Fig. 2(a)] and the root mean square (rms) roughness is 2.6 nm. After growing 3- $\mu$ m-thick GaN at 1050 °C, lots of dots remained with a rms roughness of 1.8 nm [Fig. 2(b)], which differs from *c*-oriented GaN on sapphire. A magnified

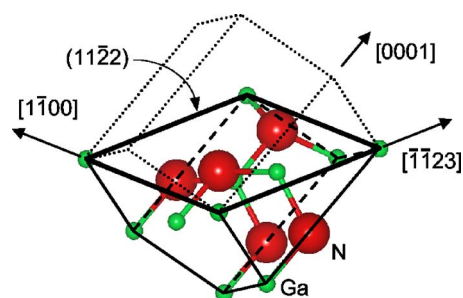


FIG. 1. (Color online) Schematic crystal structure of GaN with a (11 $\bar{2}$ 2) surface.

<sup>a)</sup>Electronic mail: funato@kuee.kyoto-u.ac.jp

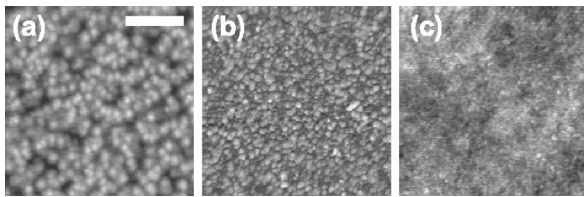


FIG. 2. Surface morphologies of (a)  $(11\bar{2}2)$  GaN substrate and GaN homoepitaxial layers grown at (b) 1050 °C and (c) 975 °C. The peak-to-valley distances are (a) 13.9 nm, (b) 9.9 nm, and (c) 1.0 nm. The scale bar represents 200  $\mu\text{m}$ .

AFM image (not shown) suggests that facets form around the dots. Because the facet structure generally depends on the growth temperature, other temperatures were examined. Consequently, we found that a lower temperature of 975 °C provides atomically flat surfaces for  $(11\bar{2}2)$  GaN and an example is shown in Fig. 2(c). As shown, the dots are replaced by fine structures and the rms roughness is as low as 0.16 nm. Cross sectional analysis indicated that the step height of the fine structures is close to the  $(11\bar{2}2)$  layer spacing (0.136 nm). A clue to understanding why a lower temperature is suitable for growth on the  $(11\bar{2}2)$  plane can be found in conventional regrowth techniques on patterned  $c$ -oriented GaN where the  $\{11\bar{2}2\}$  facets tend to appear at low temperatures.<sup>13,14</sup>

In order to assess the fundamental optical properties of the GaN homoepitaxial layer grown at the optimal temperature (975 °C), photoluminescence (PL) and reflectance were measured at 10 K. For the PL measurement, the sample was excited by a He–Cd laser (325 nm). The reflectance measurements were performed using a Xe lamp at a normal incidence on the sample surface. Both PL and reflectance were detected through a 1 m monochromator coupled with a photomultiplier tube. The resolution is  $\sim 0.08$  meV at 350 nm. To see the optical anisotropy effect, a polarizer was set between the sample and detector. Figure 3 shows the PL and reflectance spectra where the reflectance was measured for the light with the electric field vector ( $E$ ) parallel to the  $[1\bar{1}00]$  direction ( $\perp c$ ) or the  $[\bar{1}\bar{1}23]$  direction. In the reflectance spectra, transitions involving ground-state  $A$ ,  $B$ , and  $C$  excitons are well resolved at 3.4802, 3.4848, and 3.503 eV

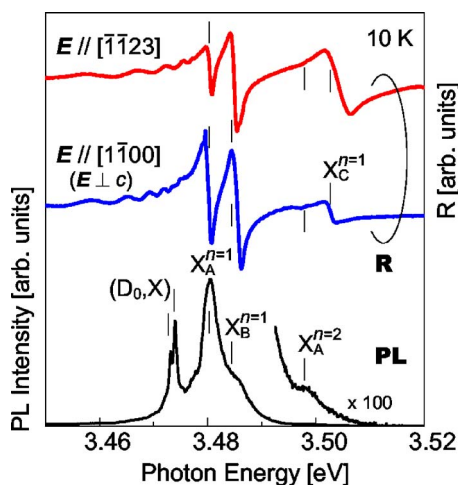


FIG. 3. (Color online) PL and reflectance spectra of the GaN homoepitaxial layer acquired at 10 K.

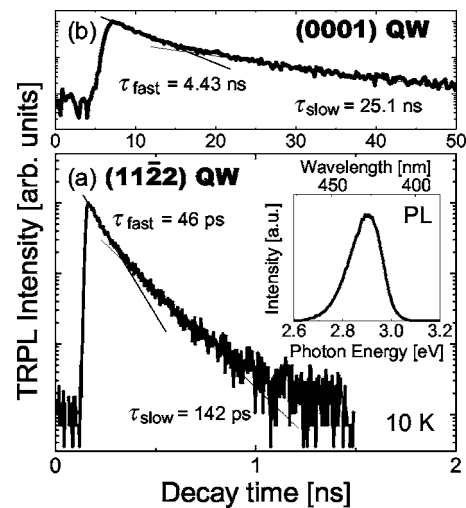


FIG. 4. PL decays for (a)  $(11\bar{2}2)$  MQW and (b)  $(0001)$  QW at 10 K. The inset of (a) is the PL spectrum.

(denoted  $X_A^{n=1}$ ,  $X_B^{n=1}$ , and  $X_C^{n=1}$ ), respectively. These quantities closely match those reported for bulk GaN,<sup>15–17</sup> suggesting a negligible strain in our homoepitaxial layers. A weak signal denoted as  $X_A^{n=2}$  at 3.4977 eV is derived from  $n=2$  free  $A$  excitons. Comparing the two observed reflectance spectra, it is found that the  $X_A^{n=1}$  signal is stronger for the  $[1\bar{1}00]$  direction and  $X_C^{n=1}$  is stronger for the  $[\bar{1}\bar{1}23]$  direction, both of which are well accounted for by considering the crystal symmetry of the  $(11\bar{2}2)$  plane. For PL, emissions from  $X_A^{n=2}$ ,  $X_B^{n=1}$ ,  $X_A^{n=1}$ , and the neutral donor-bound exciton ( $D_0, X$ ) are observed.  $X_A^{n=1}$  is dominant, indicating high optical qualities. The  $(D_0, X)$  emission is clearly split into a doublet at 3.4738 and 3.4729 eV; the relative intensities depend on the growth conditions and therefore are attributed to different donor species. A fit using two Lorentzian curves gives an identical linewidth of 0.6 meV, which is comparable to those of most state of art homoepitaxial or bulk GaN.<sup>15–17</sup>

A five-period InGaN/GaN MQW was fabricated on this high quality GaN homoepitaxial layer. The x-ray diffraction profile of the MQW consisted of satellite peaks, by which the well and barrier layer thicknesses were evaluated to be 3.4 and 11.3 nm, respectively. As for the optical properties, the carrier recombination dynamics interest us because the radiative lifetime, which is inversely proportional to the transition probability, is a good index of the strength of the internal electric field. Therefore, time-resolved PL measurements were conducted at 10 K, which is a temperature where non-radiative recombinations are negligible. The excitation pulses were from a frequency doubled Ti:sapphire laser with a wavelength of 380 nm to selectively excite InGaN wells and a power density as low as 470 nJ/cm<sup>2</sup>. The PL was detected by a streak camera. Figure 4(a) shows the time-integrated PL spectrum in the inset and a PL decay curve monitored at the 428 nm emission peak. For comparison, a PL decay curve measured for a  $(0001)$  InGaN/GaN QW, which emits a similar wavelength, is plotted in Fig. 4(b). Both decay curves have fast and slow lifetimes and can be fitted by double exponential curves. For the  $(11\bar{2}2)$  MQW, the fast and slow lifetimes are estimated to be 46 and 142 ps, respectively, and are nearly independent of the monitoring wavelength within the PL spectrum. This observation is dif-

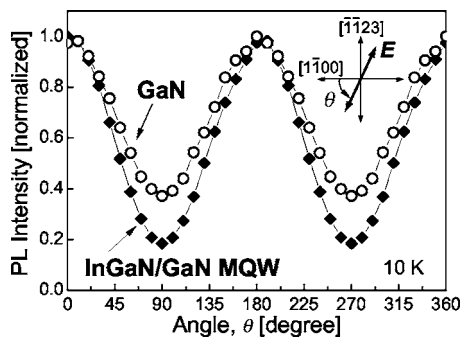


FIG. 5. PL polarization property of the  $(1\bar{1}\bar{2}\bar{2})$  GaN homoepitaxial layer (open circles) and InGaN/GaN MQW (closed squares) at 10 K.  $\theta=0^\circ$  corresponds to the  $[1\bar{1}00]$  direction, while  $\theta=90^\circ$  corresponds to the  $[\bar{1}\bar{1}23]$  direction.

ferent from conventional InGaN/GaN QWs because recombination dynamics in conventional InGaN/GaN QWs are well explained by weakly localized excitons and the PL lifetimes decrease as the wavelength decreases in the short-wavelength tail of the spectra. Analysis of this wavelength dependence is currently in progress. On the other hand, for the (0001) QW, the lifetimes are 4.43 and 25.1 ns, which are two orders of magnitude larger than in the  $(1\bar{1}\bar{2}\bar{2})$  MQW. Because the PL linewidth of the (0001) QW is narrower than that of the  $(1\bar{1}\bar{2}\bar{2})$  MQW, potential fluctuations may be less in the (0001) QW, and consequently, the radiative recombination process should be faster. Nevertheless, the lifetimes for the  $(1\bar{1}\bar{2}\bar{2})$  MQW are much shorter, indicating a higher transition probability in this semipolar MQW due to the significantly weakened internal electric field.

Due to the low crystalline symmetry of the  $(1\bar{1}\bar{2}\bar{2})$  plane, the PL should exhibit polarization anisotropy. Our calculation based on the  $\mathbf{k}\cdot\mathbf{p}$  theory predicts the following: (a) PL is polarized along the  $[1\bar{1}00]$  direction ( $\perp c$ ), (b) unstrained GaN has a polarization degree of 0.56, and (c) strained InGaN on unstrained GaN shows a larger polarization degree where the polarization degree is defined as  $(I_{[1\bar{1}00]} - I_{[\bar{1}\bar{1}23]}) / (I_{[1\bar{1}00]} + I_{[\bar{1}\bar{1}23]})$ . The polarizations were measured for our  $(1\bar{1}\bar{2}\bar{2})$  GaN homoepitaxial layer and InGaN/GaN MQW at 10 K and Fig. 5 shows the results. For the GaN layer, to avoid the overlap with the  $X_B^{n=1}$  emission, the polarization was monitored on the lower energy side of the  $X_A^{n=1}$  emission (3.4792 eV). It is clear that both the GaN layer and InGaN/GaN MQW emit strongly polarized light. The polarization degrees were calculated to be 0.46 and 0.69, respectively, which agree well with the prediction and indicate the high optical quality of our samples. The larger polarization degree for the MQW is due to the anisotropic com-

pressive strain induced by the lattice mismatch between GaN and InGaN.

To summarize, GaN and InGaN/GaN MQW were grown on semipolar  $\{1\bar{1}\bar{2}\bar{2}\}$  GaN bulk substrates. The GaN homoepitaxial layer had an atomically flat surface and excitonic transitions governed the optical properties. The InGaN/GaN MQW grown on the GaN homoepitaxial layer involved carrier radiative lifetimes of  $\sim 100$  ps, which are much shorter than conventional  $c$ -oriented QWs and were attributed to the weakened internal electric field. The emissions from both GaN and the MQW indicate that the polarization ability is due the crystal symmetry.

The authors acknowledge A. Kaneta (Kyoto Univ.) for his help in the experiments and data analyses. This work is partially supported by Grants for Regional Science and Technology Promotion from the Ministry of Education, Culture, Sports, Science and Technology and the 21st Century COE Program (No. 14213201). Figure 1 was drawn with VENUS developed by Drs. Dilanian and Izumi.

- <sup>1</sup>F. Bernardini and V. Fiorentini, Phys. Status Solidi B **216**, 391 (1999).
- <sup>2</sup>P. Waltereit, O. Brandt, A. Trampert, H. T. Grahn, J. Menniger, M. Ramsteiner, M. Reiche, and K. H. Ploog, Nature (London) **406**, 865 (2000).
- <sup>3</sup>B. A. Haskell, F. Wu, S. Matsuda, M. D. Craven, P. T. Fini, S. P. DenBaars, J. S. Speck, and S. Nakamura, Appl. Phys. Lett. **83**, 1554 (2003).
- <sup>4</sup>K. Nishizuka, M. Funato, Y. Kawakami, Sg. Fujita, Y. Narukawa, and T. Mukai, Appl. Phys. Lett. **85**, 3122 (2004).
- <sup>5</sup>K. Nishizuka, M. Funato, Y. Kawakami, Y. Narukawa, and T. Mukai, Appl. Phys. Lett. **87**, 231901 (2005).
- <sup>6</sup>M. Funato, T. Kotani, T. Kondou, Y. Kawakami, Y. Narukawa, and T. Mukai, Appl. Phys. Lett. **88**, 261920 (2006).
- <sup>7</sup>R. Sharma, P. M. Pattison, H. Masui, R. M. Farrel, T. J. Baker, B. A. Haskell, F. Wu, S. P. DenBaars, J. S. Speck, and S. Nakamura, Appl. Phys. Lett. **87**, 231110 (2005).
- <sup>8</sup>A. Chakraborty, T. J. Baker, B. A. Haskell, F. Wu, J. S. Speck, S. P. DenBaars, S. Nakamura, and U. K. Mishra, Jpn. J. Appl. Phys., Part 2 **44**, L945 (2005).
- <sup>9</sup>T. J. Baker, B. A. Haskell, F. Wu, J. S. Speck, and S. Nakamura, Jpn. J. Appl. Phys., Part 2 **45**, L154 (2006).
- <sup>10</sup>T. Takeuchi, H. Amano, and I. Akasaki, Jpn. J. Appl. Phys., Part 1 **39**, 413 (2000).
- <sup>11</sup>S.-H. Park, J. Appl. Phys. **91**, 9904 (2002).
- <sup>12</sup>M. Funato, M. Ueda, Y. Kawakami, Y. Narukawa, T. Kosugi, M. Takahashi, and T. Mukai, Jpn. J. Appl. Phys., Part 2 **45**, L659 (2006).
- <sup>13</sup>H. Marchand, J. P. Ibbetson, P. T. Fini, S. Keller, S. P. DenBaars, J. S. Speck, and U. K. Mishra, J. Cryst. Growth **195**, 328 (1998).
- <sup>14</sup>K. Hiramatsu, K. Nishiyama, M. Onishi, H. Mizutani, M. Narukawa, A. Motogaito, H. Miyake, Y. Iyechika, and T. Maeda, J. Cryst. Growth **221**, 316 (2000).
- <sup>15</sup>K. Kornitzer, T. Ebner, M. Grehi, K. Thonke, R. Sauer, C. Kirchner, V. Schwegler, M. Kamp, M. Leszczynski, I. Grzegory, and S. Porowski, Phys. Status Solidi B **216**, 5 (1999).
- <sup>16</sup>K. Torii, T. Deguchi, T. Sota, K. Suzuki, S. Chichibu, and S. Nakamura, Phys. Rev. B **60**, 4723 (1999).
- <sup>17</sup>B. J. Skromme, K. C. Palle, C. D. Poweleit, H. Yamane, M. Aoki, and F. J. DiSalvo, Appl. Phys. Lett. **81**, 3765 (2002).